Astron. Astrophys. 362, 959–967 (2000)

ASTRONOMY AND ASTROPHYSICS

BVI photometry and integrated spectroscopy of the very young open clusters Ruprecht 119, NGC 6318 and BH 245⋆

A.E. Piatti[1], **E. Bica**[2], **and J.J. Clariá**[1]

[1] Observatorio Astronómico, Laprida 854, 5000 Córdoba, Argentina
[2] Universidade Federal do Rio Grande do Sul, Depto. de Astronomía, CP 15051, Porto Alegre, 91500-970, Brazil

Received 9 August 2000 / Accepted 20 September 2000

Abstract. We present CCD BVI observations obtained for stars in the fields of the unstudied or poorly studied open clusters Ruprecht 119, NGC 6318, and BH 245 projected close to the direction towards the Galactic centre. We measured V magnitude and $B-V$ and $V-I$ colours for about 600 stars reaching down to $V\sim19$ mag. From the analysis of the colour magnitude diagrams, we confirmed the physical reality of the clusters and derived their reddening, distance and age for the first time. In addition, we obtained flux-calibrated integrated spectra in the range 3500-9200 Å for the cluster sample. Using the equivalent widths of the Balmer lines and comparing the cluster spectra with template spectra we derive both foreground reddening and age. The photometric and spectroscopic results reveal that the three studied objects are very young open clusters with ages ranging between 10 and 15 Myr, which have already undergone the HII region evolutionary phase and are dominated by the upper MS stars. The clusters, located between 1.1 kpc and 3.3 kpc from the Sun, are affected by different amounts of interstellar visual absorption ($2.4\leq \mathrm{A}_v\leq 7.0$). In particular, BH 245 turned out to be a highly reddened open cluster located at a distance of scarcely 1.1 kpc.

Key words: techniques: photometric – techniques: spectroscopic – Galaxy: open clusters and associations: general – Galaxy: open clusters and associations: individual: BH 245, NGC 6318, Ruprecht 119

1. Introduction

Galaxy disks constitute important subsystems in many galaxies, in addition to halos and bulges, which tell us about the chemical evolution history of such galaxies. In the case of the Milky Way, the disk plays an important role in the Galaxy history, connecting its formation to the present during approximately 2/3 of the Galaxy life. In this framework, the Galactic open cluster system provides a valuable tool to investigate the dynamical and chemical evolution of the Galactic disk, since open clusters are found throughout the whole disk and roughly spread over its full age range. In addition, open clusters can supply accurate ages, distances and metallicities in a more expeditive way than individual stars. Colour-magnitude diagrams (CMDs) have long been used to derive their fundamental parameters as well as to put new observational constraints on the stellar evolutionary models. In particular, open clusters located towards the Galactic centre are of great interest as they offer the possibility to explore in detail the structure and evolution of the inner disk more precisely.

The advent of CCD detectors and computing facilities has allowed one to build up deeper and more populous CMDs of relatively small angular size objects. Indeed, the success of CCD technique results are particularly evident in studies of compact star clusters. This is why during the last decade numerous works of faint clusters projected in obscure and/or crowded fields have appeared. CMDs of such clusters, however, often suffer from high interstellar absorption, field star contamination, or both effects combined, which need to be corrected before deriving any cluster parameter. At times CMDs contain two star sequences - one of them being the genuine cluster sequence - or even only one sequence of field stars corresponding on the sky to a chance grouping. The presence of an apparent stellar concentration in the sky is not at all a sufficient condition for inferring that we are dealing with a physical cluster. This criterion is probably valid in the case of globular clusters or very concentrated open clusters. But, for most of the apparent stellar concentrations it is necessary to supplement the photometric data with spectroscopic and, if possible, also kinematical data (proper motion and/or radial velocities) in order to confirm their real physical existence. However, since the number of open clusters with available spectroscopic and kinematical data is much smaller than those which have photometric data, frequently the latter is the only set of data from which the existence of an open cluster may be inferred from. Differences in the star density in some region of the sky can be caused either by the presence of a genuine open cluster, by a random fluctuation of the star density in that region, by the presence of interstellar material inhomogeneously distributed, or by some combination of these three

Send offprint requests to: A.E. Piatti (andres@mail.oac.uncor.edu)

⋆ Based on observations made at the University of Toronto (David Dunlap Observatory) 24inch telescope, Las Campanas, Chile, and at the Complejo Astronómico El Leoncito, which is operated under agreement between the Consejo Nacional de Investigaciones Científicas y Técnics de la República Argentina and the National Universities of La Plata, Córdoba, and San Juan, Argentina.

effects. We recall that more than half of the 1200 presently catalogued open clusters have been poorly studied or not studied yet. Therefore, the confirmation of the physical reality of cluster candidates alone, is a valuable contribution to our knowledge of the open cluster system.

The present study is part of an ongoing long-term program which consists in obtaining CCD photometric and spectroscopic data of southern open cluster candidates preferably projected towards the inner Galactic disk (galactocentric distances ≤ 8 kpc). The candidates were selected taking into account the following criteria: (i) first, objects from early cataloguing studies for which little or no information is available, together with some control clusters. (ii) The angular sizes of the clusters were basically limited to $4'$, in order to facilitate the observation with CCD detectors covering relatively small fields, and also to allow one to obtain long slit integrated spectra with background sampling (some objects with larger angular sizes were also added) and (iii) according to the stellar density and morphology of the candidates they were expected to be genuine clusters.

In this work we present the results obtained for three of the selected open clusters, namely: Ruprecht 119 (OCl-963, α_{2000}=$16^h28^m15^s$, δ_{2000}=-51°30′14″; l=333°.27, b=-1°.88), NGC 6318 (OCl-1004, α_{2000}=$17^h16^m12^s$, δ_{2000}=-39°25′30″; l=347°.90, b=-0°.69), and BH 245 (α_{2000}=$17^h46^m15^s$, δ_{2000}=-29°42′01″; l=359°.41, b=-0°.51). Ruprecht 119 is located in Norma, NGC 6318 in Scorpius and BH 245 in Sagittarius, all projected close to the Galactic centre. Notice that the original coordinates of NGC 6318 appearing in early catalogs are off, the correct ones appeared in van den Bergh & Hagen (1975, hereinafter vdBH75), therein as BH 218, and in Lauberts (1982, therein indicated both as NGC 6318 and ESO333-SC1). Only Ruprech 119 has some information available. Moffat & Vogt (1973, hereinafter MV73) observed 13 stars in the field of Ruprecht 119 using UBV photoelectric photometry and concluded that the object is not a cluster. On the other hand, vdBH75 identified for the first time a questionable object visible in red plates and not visible in blue plates, which they catalogued as a probable very poor cluster (BH 245).

This paper is structured as follows: in Sect. 2 we present the observations and briefly describe the reduction procedures. In Sect. 3 we present the results obtained from the photometric and spectroscopic data, respectively, and discuss the adopted cluster parameters. Finally, Sect. 4 summarizes the main conclusions of this work.

2. Observations and reductions

CCD BVI images in the fields of Ruprecht 119, NGC 6318 and BH 245 were obtained during three photometric nights in September 1994 and June-July 1995, respectively, using the 24-inch telescope of the University of Toronto Southern Observatory (Las Campanas Observatory, Chile). In both runs we employed the same PM 512x512 METACHROME coated CCD to give improved blue response. As the scale on the chip is $0''.45$ per pixel, the sky covered by a single frame is about $4'$x$4'$. The observations were supplemented with a series of 10 bias and 10 skyflats during the sunsets and 10 domeflats at the end of each night to calibrate the CCD instrumental signature. During the two observing runs the typical seeing was $1''.5$. The sequence of observations per filter for the three objects is listed in Table 1, while their schematic finding charts in the V-passband are shown in Fig. 1. Observations of 10–14 stars in the Selected Area standard fields (Landolt 1992) covering a wide range in colour ($0.2 \leq V-I \leq 1.9$) were also taken nightly. The airmass values for both program and standard fields were always smaller than 1.2.

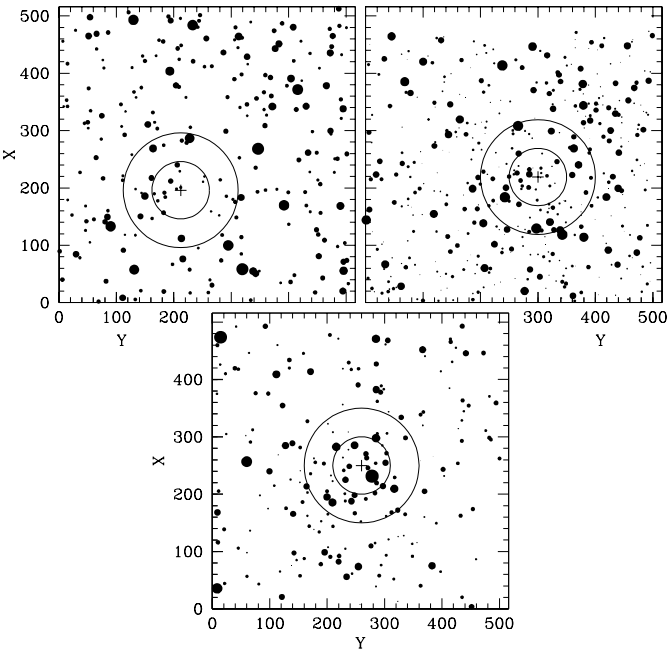

Fig. 1. Schematic finding charts for the fields of Ruprecht 119 (top-left), NGC 6318 (top-right), and BH 245 (bottom). A cross indicates the adopted cluster centre. Two concentric circles of $22''.5$ and $45''.0$ radii are also shown. North is up and East is to the left.

The observations were reduced at the Astronomical Observatory of the National University of Córdoba, Argentina, using the IRAF[1] routines. The extinction corrected instrumental magnitudes b, v and i were obtained following the reduction procedure described by Piatti et al. (1999) and transformed to the standard system from the following relations:

$$b_{j,n} = b_1 + V + (B-V) + b_2(B-V), \quad (1)$$

$$v_{k,n} = v_1 + V + v_2(B-V), \quad (2)$$

$$i_{l,n} = i_1 + V - (V-I) + i_2(V-I), \quad (3)$$

where V, $(B-V)$ and $(V-I)$ are the standard magnitude and colours. Eqs. (1) to (3) were simultaneously solved by least squares for each night n, the rms errors being ≤ 0.01 mag in all the passbands. The resulting coefficients listed in Table 2 were then used to derive magnitude and colours of all the stars

[1] IRAF is distributed by the National Optical Astronomy Observatories, which is operated by the Association of Universities for Research in Astronomy, Inc., under contract with the National Science Foundation

Table 1. Journal of observation.

Object	Date (UT)	Filter	Exposures	seeing ($''$)
Ruprecht 119	1994 September 5	B	1x60 sec, 2x250 sec	1.7
		V	1x60 sec, 1x90 sec, 1x150 sec	1.4
		I	1x15 sec, 1x30 sec, 1x60 sec	1.4
NGC 6318	1995 June 29	B	1x60 sec, 2x600 sec	1.4
		V	1x60 sec, 2x300 sec	1.5
		I	1x10 sec, 2x30 sec	1.4
BH 245	1995 July 3	B	1x60 sec, 1x600 sec, 1x900 sec	1.8
		V	1x60 sec, 2x600 sec	1.6
		I	1x2 sec, 2x60 sec	1.6

Table 2. Transformation coefficients.

Date (UT)	b_1	b_2	v_1	v_2	i_1	i_2
1994 September 5	6.300	-0.017	5.920	-0.052	5.230	-0.055
	$\pm$0.011	$\pm$0.007	$\pm$0.010	$\pm$0.008	$\pm$0.010	$\pm$0.010
1995 June 29	7.267	-0.043	7.051	-0.039	6.551	-0.084
	$\pm$0.009	$\pm$0.004	$\pm$0.009	$\pm$0.010	$\pm$0.011	$\pm$0.011
1995 July 3	7.256	-0.085	7.053	-0.019	6.531	-0.075
	$\pm$0.011	$\pm$0.006	$\pm$0.010	$\pm$0.011	$\pm$0.013	$\pm$0.012

measured for different independent combinations of BVI images. We thus generated three independent tables per program object containing a running star number, the X and Y coordinates, the V magnitude, the $B-V$ and $V-I$ colours, and the observational errors provided by the IRAF.INVERFIT task $\sigma(V)$, $\sigma(B-V)$, and $\sigma(V-I)$. These three tables were finally combined averaging the values for stars which appear in more than a single table. This procedure allowed us to obtain the individual photometric internal errors and to detect any anomalous value as well. The final tables are available upon request to the first author. A comparison of our CCD photometry with MV73 for 7 stars in common in the field of Ruprecht 119 yields $\Delta(V_{MV73}-V_{CCD}) = -0.02 \pm 0.07$ and $\Delta((B-V)_{MV73}-(B-V)_{CCD}) = 0.06 \pm 0.04$. However, Kozok (1985) obtained three accurate measurements for star # 6 of MV73 and the difference between both photometries yields $\Delta(V_{MV73}-V_K) = -0.04$ and $\Delta((B-V)_{MV73}-(B-V)_K) = 0.05$, which suggests that the zero points of MV73's photometry could be slightly shifted. For this reason, we decided not to apply any zero point correction to our photometry of Ruprecht 119.

We also obtained integrated spectra for the three objects under discussion with a REOSC spectrograph and a Tek 1024x1024 CCD (1 pixel=24 μm) attached to the 2.15 m telescope at the Complejo Astronómico El Leoncito (CASLEO, Argentina) during a run in May 1995. The observations were carried out scanning the slit across the objects in the north-south direction in order to properly sample the cluster stellar content and the background regions. The total field along the slit was $4'.7$. A grating of 300 lines/mm was used in two different set-ups, namely "blue nights" and "red nights". During the blue nights, we obtained spectra ranging from 3500 to 7000 Å with an average dispersion in the observed region of 140 Å/mm (3.46 Å/pixel). The slit width was $4''.2$ resulting in an average resolution of 14 Å, according to the FWHM of the He-Ar comparison lamps. During the red nights, we obtained spectra from 5800 to 9200 Å with a similar dispersion (3.36 Å/pixel) and a resolution of 17 Å (same slit width). To eliminate second order contamination an OG 550 filter was employed. Exposures of 15 minutes were taken until reach a total of 45 minutes for Ruprecht 119 and one hour for the remaining two objects in the blue and red ranges, respectively; the resulting S/N ratios ranging between 15 and 50. In addition, spectra of standard stars to derive flux calibrations were also obtained. In the blue range we used the standard stars LTT 4364, EG 274 and LTT 7379 (Stone & Baldwin 1983), whereas in the red range we added to the standard list the hot dwarf star HD 160233 (Gutiérrez-Moreno et al. 1988) with the aim of applying corrections for telluric emission bands. The integrated spectra were reduced at the Astronomical Observatory of Córdoba following the precepts outlined by Piatti et al. (1998a). For the reduction we used He-Ar comparison lamp spectra obtained between and after the object observations as well as bias, and dome, twilight sky and tungsten lamp flat-fields obtained nightly.

3. Analysis and discussion

3.1. Photometric analysis

The observed $(V, B-V)$ and $(V, V-I)$ CMDs are shown in Figs. 2a and 2b, respectively, wherein the reddening vector for E(B-V) = 0.5, assuming A_v=3.0E(B-V) and E(V-I)/E(B-V) = 1.25 (Walker 1985, Straižys 1990), is also drawn. All CMDs exhibit star sequences with overall properties and some specific peculiarities. A common feature is that the upper part of star sequences is not parallel to the reddening vector but rather follows the envelope of Main Sequences (MSs) of relatively young open clusters. This feature is less obvious for BH 245 whose $(V, B-V)$ diagram only shows two very sparce groups of stars, which become stellar sequences in the $(V, V-I)$ plane. Field star sequences have a lower envelope with a smaller curvature than that of the Zero Age Main Sequence (ZAMS). This envelope does not depend on the space star density but on the parameters of the interstellar extinction, namely $R = A_v/E(B-V)$

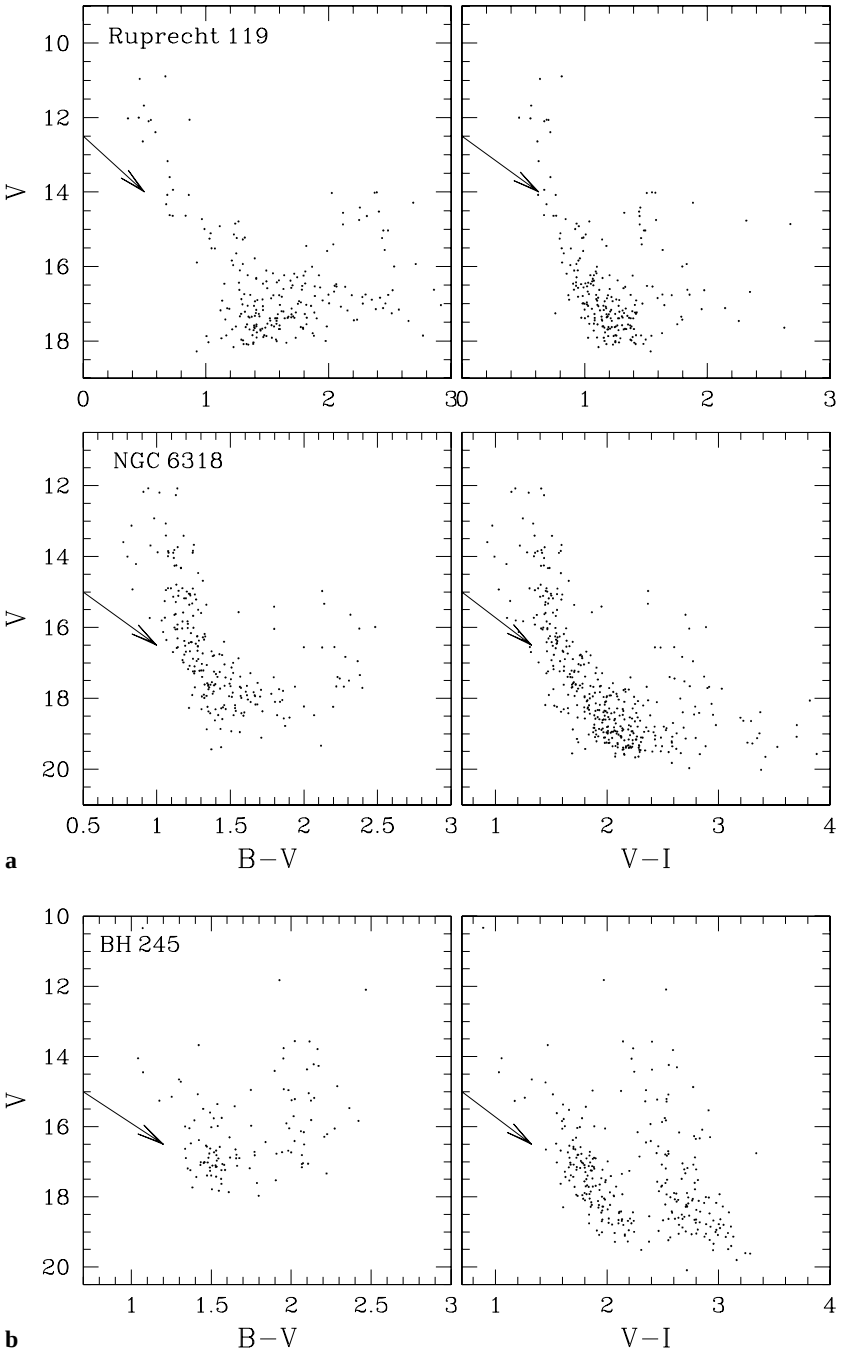

Fig. 2. a (V,$B-V$) and (V,$V-I$) diagrams of stars in the fields of Ruprecht 119 (top) and NGC 6318 (bottom); **b** (V,$B-V$) and (V,$V-I$) diagrams of stars in the fields of BH 245. The direction and size of the reddening vector for E(B-V)=0.5 mag, assuming A_v=3.0E(B-V) and E(V-I)=1.25E(B-V), are also shown.

(Burki & Maeder 1973). The redder star sequence in the field of BH 245 seems to correspond to the object because it has a wider magnitude range in the ($V, V-I$) plane (with fainter and brighter stars) and it is not as faint as the bluer star group in the ($V, B-V$) diagram. The redder sequence is also not only less populous than the bluer one, in good agreement with the very poor star richness quoted by vdBH75, but also more tilted with respect to the direction of the reddening vector. The remarkable difference in the number of stars between both CMDs is mainly due to reddening effects.

The CMDs of Ruprecht 119 present a long MS which extends between the eleventh down to the eighteenth magnitude, largely superseding the photometry of MV73 which reaches $V \sim 12.5$ mag. This is probably the main reason why Ruprecht 119 was considered not to be a cluster by MV73. The brighter portion of the cluster MS is particularly well defined, while there are two apparent gaps in the ($V, B-V$) diagram at ($V, B-V$) $\approx$ (13.5, 0.6) and (16.0, 0.8). These gaps may be indicators either of differential reddening or of evolutionary effects (see, e.g. Canterna et al. 1979). Differential reddening could be caused by the presence of dust within the cluster because the bluest point of the MS is not as red as it would be expected if the cluster suffered from a high interstellar absorption. Note also that the MS in the ($V, V-I$) diagram is not

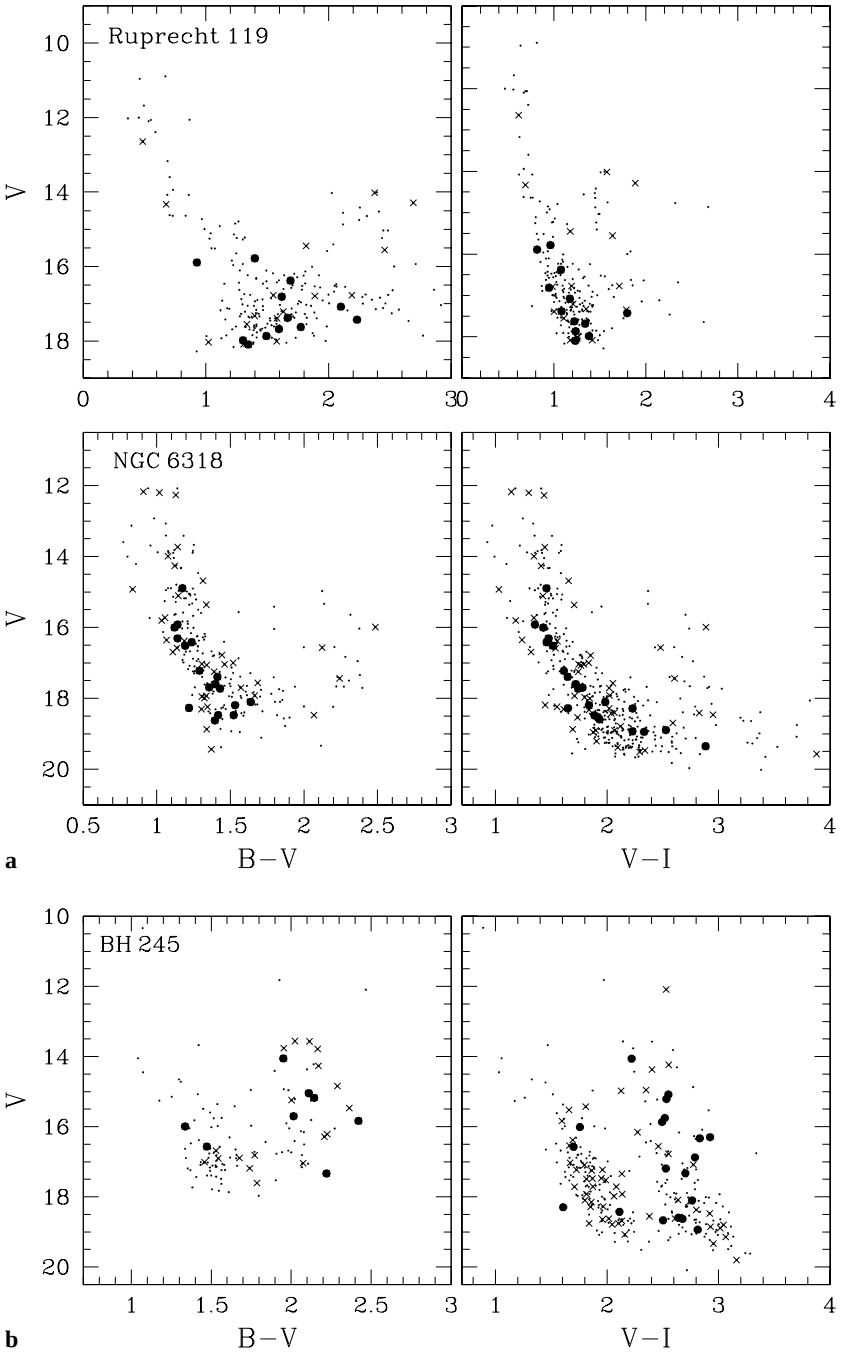

Fig. 3. a Colour-magnitude diagrams of stars in the fields of Ruprecht 119 (top) and NGC 6318 (bottom): all measured stars (dots), circular extraction for r<22″.5 (filled circles) and r<45″.0 (crosses) are superimposed; **b** Colour-magnitude diagrams of stars in the fields of BH 245: symbols same as **a**.

as broad as that in the $(V, B-V)$ diagram. Anyway, both hypotheses for the gaps origin indicate that Ruprecht 119 should be a young cluster. The CMDs of NGC 6318 also reveal the presence of a well-defined MS, the $(V, V-I)$ diagram being at least one magnitude deeper than the $(V, B-V)$ diagram, which is essentially due to reddening effects. Both CMDs exhibit no significant star field contamination.

With the aim of finding out whether stars in the field of BH 245 are distributed in the CMDs along a sequence or randomly, we first determined the cluster centre and then carried out circular extractions of stars located within 50 (22″.5) and 100 (45″.0) pixels. The cluster centre was determined from star density profiles built in the X and Y directions using all the measured stars, and from the geometrical centre taken from the corresponding finding chart. The adopted weighted value for the position of the cluster centre turned out to be (X_c, Y_c) = (250, 260). For completeness purposes we repeated the same analysis for Ruprecht 119 and NGC 6318, the resulting cluster centres being (196, 212) and (219, 300), respectively. Figs. 3a and 3b show the extracted CMDs, wherein filled circles and crosses represent stars within 50 and 100 pixels from their cluster centres, respectively. The smallest circular extraction allows us to know which are the CMD regions where the fiducial cluster sequences are located, while the largest circular extractions rep-

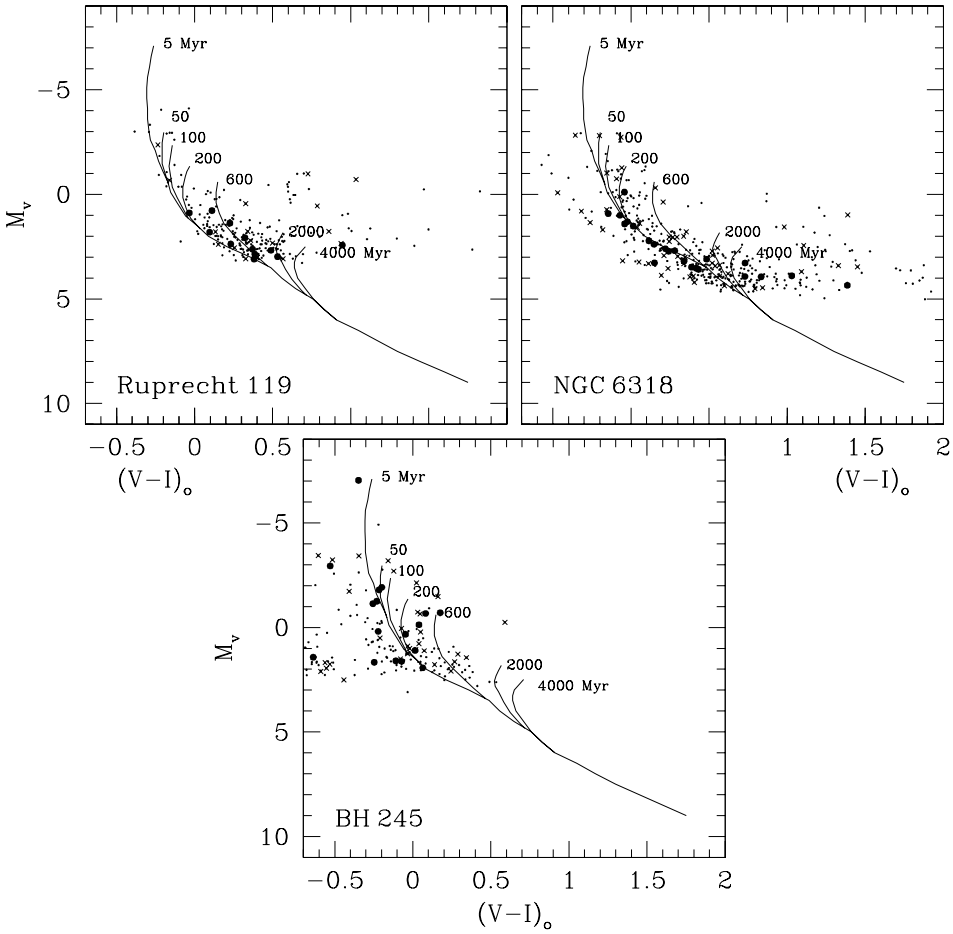

Fig. 4. M_v vs $(V\text{-}I)_o$ diagrams with the isochrones of Piatti et al. (1998b) superimposed. Symbols are as in Fig. 3.

Table 3. Cluster fundamental parameters derived from the CMDs analysis.

Cluster	E(B-V)	σ	E(V-I)	σ	V-M_v	σ	Age Myr
Ruprecht 119	0.80	0.05	0.85	0.05	15.0	0.5	5–50
NGC 6318	1.25	0.05	1.55	0.05	15.5	0.5	5–50
BH 245	2.25	0.05	2.65	0.05	17.0	0.5	5–50

resent a compromise between minimizing the unavoidable field star contamination and maximizing the number of cluster stars. As can be seen, most of the stars located within 50 pixels from the centre of BH 245 are distributed along the red sequence, in good agrement with the description of this object given by vdBH75. Based on this result, we conclude that BH 245 is a genuine open cluster which could be few Myrs old as judged from the steepness of its MS. Circular extractions for Ruprecht 119 and NGC 6318 allowed us only to trace the fiducial sequences for the cluster core regions, since their CMDs are clearly dominated by their MS stars. Particularly, circular extractions of Ruprecht 119's CMDs did not result in a clear tracing of its MS because the object is probably more extended than the total field covered by the CCD (cluster angular diameter = $6'.2$, Alter et al., 1970).

We then determined the cluster reddening values, distances and ages by fitting the cluster MSs in the $(V, B-V)$ and $(V, V-I)$ diagrams to the ZAMS of Schmidt-Kaler (1982) and Piatti et al. (1998b), respectively. Bearing in mind that MSs alone can satisfactorily be fitted using different combinations of reddening and distance modulus, especially for young open clusters, we decided to use as reference the E(B-V) colour excesses and ages provided by the spectroscopic analysis (see Sect. 3.2). Firstly, we used spectrocopic E(B-V) colour excesses and the Schmidt-Kaler's ZAMS to derive distance moduli, which in turn were used to determine E(V-I) colour excesses by fitting MSs to the Piatti et al.'s ZAMS, the ratio E(V-I)/E(B-V)=1.25 being used. Ages were also estimated by matching the cluster MSs to the empirical isochrones of Piatti et al. (1998b, Fig. 3). Secondly, using spectrocopic ages and the empirical isochrones of Piatti et al., we matched cluster MSs to the corresponding isochrone curve and derived E(V-I) colour excesses and distance moduli. Thirdly, we use the spectroscopic ages and reddenings simultaneously to enter in the age-calibrated M_v vs $(V-I)_o$ diagram to derive distance moduli and then E(B-V) colour excesses. Finally, the adopted fundamental parameters were obtained by properly combining all of the resulting values. Fig. 4 shows the empirical isochrones of Piatti et al. with the cluster MSs superimposed, while Table 3 gives in succession the E(B-V) and E(V-I) colour excesses, and the distance modulus

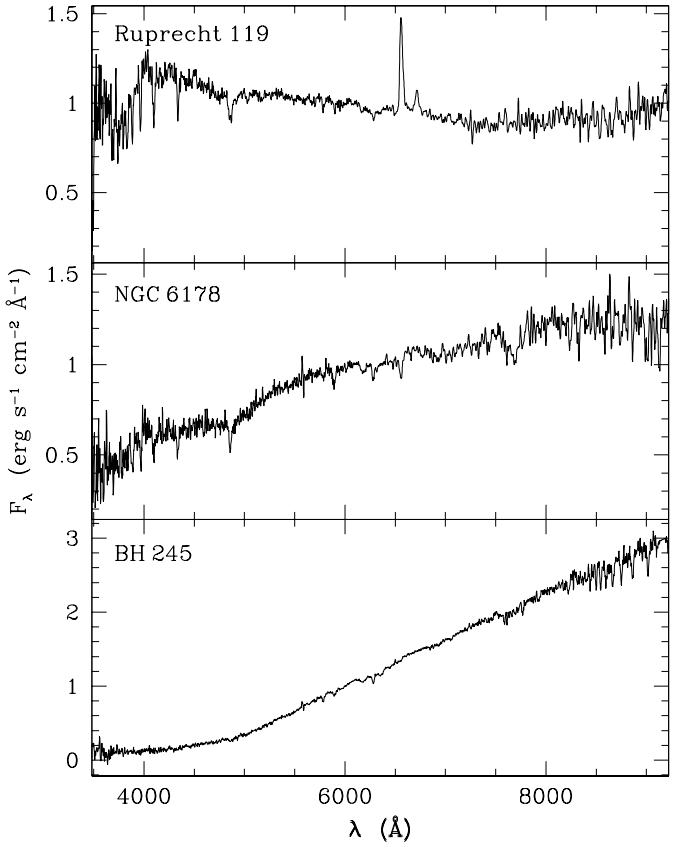

Fig. 5. Observed integrated spectra in absolute F_λ units normalized to F_λ = 1 at λ = 6000 Å.

and age for each cluster together with their corresponding errors. The last values are based on the uncertainties arising from the matching of the MSs to the ZAMSs and the age-calibrated M_v vs $(V-I)_o$ diagram. Note that we only provide an age range because of the intrinsic MS's scatter. On the other hand, using the three independent determinations for both colour excesses we derived a ratio E(V-I)/E(B-V)=1.16±0.07, which indicates that the interstellar absorption in the direction to the clusters approximately follows the normal extinction law.

3.2. Spectroscopic analysis

Fig. 5 shows the observed integrated spectra for the cluster sample normalized at λ = 6000 Å for comparison purposes. Each spectrum affected by reddening shows the combined stellar content contributing to the cluster integrated light, wherefrom each cluster age can be inferred. For the present cluster sample the different shapes and continuum slopes essentialy reflect the result of reddening effects, since the clusters are of similar ages (see Sect. 3.1). In particular, the integrated spectrum of Ruprecht 119 presents emission lines. The nebular lines [OII]$_{\lambda 3727}$ and [SII]$_{\lambda\lambda 6717,6730}$ and evidence of [NII]$_{\lambda 6584}$ in the red wing of Hα can be seen in Fig. 5. Hα itself is very strong and it probably arises from a nebular component combined to extended stellar atmospheres' emission. Nebular lines in the range 5–30 Myr can occur in the integrated cluster spectra, as observed by Santos et al. (1995) in the Magellanic Clouds clusters. They are related to winds and supernova remnants, residual emission related to fossil HII regions, or diffuse emission in HII/OB association complexes, or finally projection effects. Stars with extended atmospheres like Be also occur in a similar age range (Mermilliod 1981a,b) and they show up in the integrated spectra of Magellanic Clouds clusters (Bica et al. 1990). On the other hand, the flux value of BH 245's spectrum in the near-infrared ($\lambda\approx$ 9000 Å) relative to that at the normalization point (λ 6000 Å) results in 2.5–3.0 times higher than those of Ruprecht 119 and NGC 6318, which suggests that the cluster suffers from a significantly stronger interstellar absorption. Otherwise, if no information about the cluster age is available, a noticeable high reddening can simply be inferred from the pronounced positive slope of its spectrum. The cluster flux is roughly constant and very low in the blue range up to $\sim$ 5000 Å where it undergoes an abrupt change to increasing values until reaches a value three times higher at the end of its observed spectrum. For this reason, it is very difficult to recognize any spectral feature in the blue-visible range; the continuum slope being the most relevant characteristic along the spectrum. For $\lambda >$ 8000 Å the spectrum also shows some important residuals introduced during the subtraction procedure of atmospheric emission bands.

Integrated spectra were used to derive reddening values and ages of the cluster sample according to the precepts pointed out by Bica & Alloin (1986a, 1987). They studied integrated spectra in the visible and near-IR ranges of Galactic open and globular clusters, as well as Magellanic Clouds clusters. They examined the behaviour of metallic and Balmer line equivalent widths, as well as the continuum energy distribution in the spectral range 3700–10000 Å. They also generated a library of template cluster spectra with well-known properties. The fundamental cluster parameters were determined using the SPEED spectral analysis software (Schmidt 1988) at the Astronomical Observatory of Córdoba. First, we estimated cluster ages from equivalent widths (Ws) of Balmer lines in absorption by interpolating these values in the age calibration of Bica & Alloin (1986b), each W providing an age estimate. The ages derived from this method are reddening independent. Ws of absorption lines were measured according to the spectral windows and continuum tracings as defined in Bica & Alloin (1986a, 1987). Errors affecting the derived Ws were estimated from different measurements of the Balmer lines using high and low continuum tracings in order to take into account the spectral noise. In the case of BH 245 we could only estimate Ws for Hα and Hδ because of the low spectral signal at these wavelengths. Table 4 lists the Ws of the Balmer lines and the resulting cluster ages obtained from the average of the independent values.

We then used the ages provided by the Balmer lines to select an appropriate set of template spectra to derive cluster reddening values. The suitable template resulted to be the YA spectrum ($t \approx$ 3–6 Myr) from Santos et al. (1995), which basically corresponds to the NGC 2362 age group of Mermilliod (1981a,b). We also included in the list the YB (6–9 Myr) and YC (12–40 Myr) templates (Santos et al. 1995). These templates have flatter con-

Table 4. Cluster fundamental parameters derived from the spectroscopic analysis.

Cluster	W (Balmer)				Balmer-age	Template-age	E(B-V)
	Hα	Hβ	Hγ	Hδ	(Myr)	(Myr)	
Ruprecht 119	-14.03±0.70	4.14±0.12	4.65±0.42	6.95±0.28	15±5	3–6	0.80
NGC 6318	3.78±0.19	5.52±0.17	4.78±0.43	6.67±0.27	30±10	3–6	1.20
BH 245	0.82±0.05			4.23±0.17	$\sim$ 10	3–6	2.30

tinua than YA due to the presence of luminous evolved stars, for example supergiants, which is well-documented spectroscopically in the near-IR (Bica et al. 1990). YA, YB and YC spectra cover the spectral range between 3500 and 6000 Å where reddening effects are more noticeable. We note that not much additional reddening information would be provided if near-IR templates with similar age resolution were available. The E(B-V) colour excess of each cluster was derived by matching the observed spectrum to that of the template that most resembles it, thus making use of the full spectral distribution. The age of these templates were also taken as additional independent estimates of cluster ages. Fig. 6 shows the reddening corrected spectra of the cluster sample compared to the YA spectrum, which best matches both continuum distribution and Balmer lines simultaneously. In the figure we applied arbitrary constant offsets to the cluster spectra for comparison purposes. The general appearance of cluster spectra is very similar to that of YA, although the larger the colour excess, the noisier the spectrum for $\lambda < 4000$ Å. Balmer line intensities look similarly deep as expected because template ages were chosen from ages derived using Balmer line Ws. Note also that cluster continuum slopes ($\lambda \geq 4000$ Å) follow the trend of YA continuum quite well. If instead of YA template we had used YB, which is only ~ 3 Myr older, then the colour excesses would have been 40% lower on average. This fact shows that the matching template technique is very sensitive to both age and reddening determinations, the typical E(B-V) error being 0.05 mag. Likewise, it must be noted that template spectra are the average of integrated spectra of several different clusters so that they represent the stellar population of clusters within a limited age range. On the other hand, a cluster spectrum reflects the behaviour of the combined light coming from its members, and is consequently more dependent on stochastic effects arising from the small number of stars, as it is the case in most young open clusters in the Galaxy. The adopted template age and reddening determinations are listed in Columns 7 and 8 of Table 4.

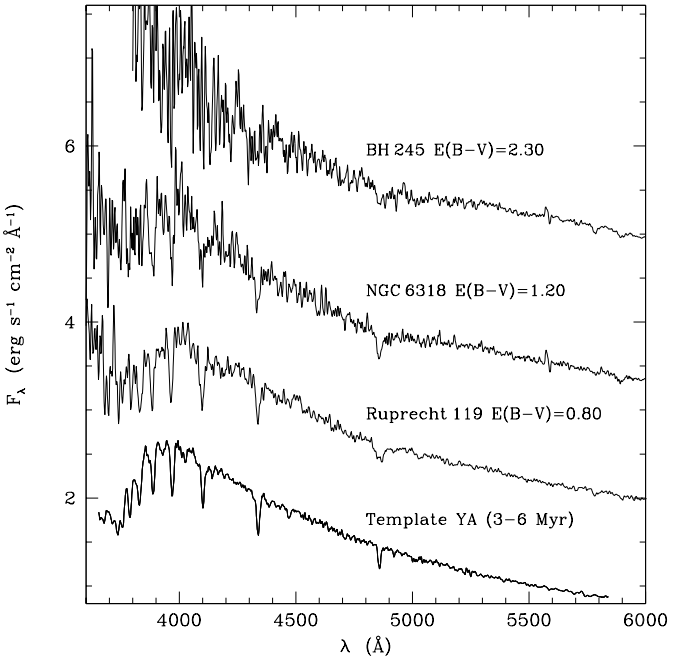

Fig. 6. Reddening-corrected integrated spectra compared with the template spectrum YA. Cluster spectra were shifted by arbitrary constants for comparison purposes.

Table 5. Adopted cluster fundamental parameters.

Cluster	E(B-V)	E(V-I)	d (kpc)	Age (Myr)
Ruprecht 119	0.80±0.05	0.85±0.05	3.3±1.0	15±10
NGC 6318	1.20±0.05	1.55±0.05	2.4±0.7	20±10
BH 245	2.25±0.05	2.65±0.05	1.1±0.3	15±10

3.3. Cluster parameters

We averaged cluster parameters derived from photometric and spectroscopic methods due to the very good agreement found between values obtained from both techniques. Table 5 lists the resulting final cluster properties. With the aim of conservatively estimating the interstellar absorption in front of the cluster, we decided to adopt the lowest value of both estimates, which closely corresponds to the mean value. Using these E(B-V) colour excesses and the apparent distance moduli of Table 3 we computed cluster distances and their corresponding uncertainties with the expression: σ(d) = 0.46[σ(V-M$_v$) + 3σ(E(B-V))]d, where σ(V-M$_v$) and σ(E(B-V)) represent the estimated errors in V-M$_v$ and E(B-V), respectively. For the E(V-I) colour excesses, we directly adopted the photometric values. Finally, cluster ages were determined averaging with the same weight the youngest and oldest ages obtained from Balmer line Ws, template matching and isochrone fitting methods. The uncertainties of the adopted ages correspond to half of the difference between the lowest and highest age values.

From the resulting ages we conclude that clusters have left the HII region phase which as a rule persists up to about 5 Myr. The integrated light of the clusters appears to be dominated by upper MS stars. No red supergiants are present in the cluster

spectra and CMD's; however, their derived ages are compatible with their occurrence. These underpopulated clusters must be suffering stochastic effects which prevent one to fully observe all products of massive star evolution expected for their ages. In addition, no evidence of substantial internal reddening was found as to infer current star formation processes. The emission of Hα in the integrated spectrum of Ruprecht 119 might be an indicator of the presence of Be stars in the cluster, which could also be responsible for the gaps seen in the $(V, B-V)$ diagram. BH 245 is very much reddened and is distant only $\approx$ 1 kpc from the Sun. A more extreme case is that of the young open cluster Westerlund 1 (Piatti et al. 1998c) which is possibly the most reddened open cluster optically observable, also located at about 1.0 kpc. Nearby individual dark clouds and complexes are known to exist in several disk directions (Cambrésy 1999), and therefore it would be important to explore in more detail the directions towards both BH 245 (Sagittarius, projected close to the Galactic centre), and Westerlund 1 in Ara, close to the Scorpius borderline.

4. Conclusions

We present new CCD BVI Johnson-Cousins photometry of stars in the fields of the unstudied or poorly studied open clusters Ruprecht 119, NGC 6318 and BH 245, which lie in the constellations of Norma, Scorpius and Sagittarius, respectively, not far from the direction towards the Galactic centre. Since our photometry reached down to V $\approx$ 19 mag, it allowed us for the first time to derive accurate cluster parameters. The present work leads to the following conclusions:

(i) We confirm the physical reality of the three objects as genuine open clusters from different circular extractions in the $(V, B-V)$ and $(V, V-I)$ diagrams and determined their reddening values, distances and ages. The observed cluster areas are not much contaminated by field stars, except that of BH 245 whose CMDs are dominated by two star sequences; the less reddened one corresponding to field stars. BH 245, barely visible in the blue, is the most reddened cluster of the sample ($A_v \approx 7$ mag).

(ii) We derive a ratio E(V-I)/E(B-V)=1.2, which indicates that the interstellar absorption along the line of sight of the clusters approximately follows the normal extinction law.

(iii) Integrated spectra for the cluster sample covering the range from 3500 to 9200 Å yielded independent determinations of cluster parameters. Balmer line equivalent widths and comparisons of the obtained spectra with template spectra provided reddening values and ages for each cluster. The spectroscopic reddening values and ages present very good agreement with the photometric ones. Ruprecht 119, NGC 6318 and BH 245 are very young objects, typically around 10–15 Myr old, which are not dominated by HII region or supergiant phases but by MS stars. Ruprecht 119 might contain some Be stars and/or residual nebular emission as inferred from both integrated spectrum and the presence of star gaps in the $(V, B-V)$ diagram.

(iv) The three studied clusters are located within the solar circle between 1.1 kpc and 3.3 kpc from the Sun. Likewise Westerlund 1 (Piatti et al. 1998c), BH 245 is a highly reddened open cluster located at about 1.0 kpc from the Sun. This high absorption is possibly caused by the presence of individual dark clouds and complexes similar to those optically mapped by Cambrésy (1999).

Acknowledgements. We acknowledge use of the CCD and data acquisition system at CASLEO, supported under US National Science Foundation grant AST 90-15827. We thank the staff and technicians at CASLEO and Las Campanas Observatory for the allocation of observing time and their kind hospitality and assistance during the runs. We also thank the referee G. Massone for his valuable comments and suggestions. We gratefully acknowledge finantial support from the argentinian institutions CONICET, Agencia Nacional de Promoción Científica y Tecnológica (ANPCyT) and SECyT (National University of Córdoba) and the Brazilian Institution CNPq.

References

Alter G., Ruprecht J., Vanỳsek J., 1970, In: Alter G., Balázs B., Ruprecht J. (eds.) Catalogue of Star Clusters and Associations. Akademiai Kiado, Budapest
Bica E., Alloin D., 1986a, A&A 162, 21
Bica E., Alloin D., 1986b, A&AS 66, 171
Bica E., Alloin D., 1987, A&A 186, 49
Bica E., Alloin D., Santos J.F.C., 1990, A&A 235, 103
Burki G., Maeder A., 1973, A&A 25, 71
Cambrésy L., 1999, A&A 345, 965
Canterna R., Perry C.L., Crawford D.L., 1979, PASP 91, 263
Gutiérrez-Moreno A., Moreno H., Cortés G., Wenderoth E., 1988, PASP 100, 973
Kozok J.R., 1985, A&AS 61, 387
Landolt A.U., 1992, AJ 104, 340
Lauberts A., 1982, The ESO/Uppsala Survey of the ESO (B) Atlas. European Southern Observatory, Garching bei München
Mermilliod J.C., 1981a, A&A 97, 235
Mermilliod J.C., 1981b, A&AS 44, 467
Moffat A.F.J., Vogt N., 1973, A&AS 10, 135 (MV73)
Piatti A.E., Bica E., Clariá J.J., 1998c, A&AS 127, 423
Piatti A.E., Clariá J.J., Bica E., 1998b, ApJS 116, 263
Piatti A.E., Clariá J.J., Bica E., 1999, MNRAS 303, 65
Piatti A.E., Clariá J.J., Bica E., Geisler D., Minniti D., 1998a, AJ 116, 801
Santos J.C.F., Bica E., Clariá J.J., et al., 1995, MNRAS 276, 155
Schmidt A., 1988, User Manual. Federal University of Santa María, Brazil
Schmidt-Kaler Th., 1982, In: Schaifers K., Voigt H.H. (eds.) Landolt-Börnstein. Numerical Data and Functional Relationships in Science and Technology. New Series, group VI, Vol. 2b, Springer Verlag, Berlin
Stone R.P.S., Baldwin J.A., 1983, MNRAS 204, 347
Straižys V., 1990, Multicolor Stellar Photometry. Pachart Publ. House, Tucson, Arizona
van den Bergh S., Hagen G.L., 1975, AJ 80, 11
Walker A.R., 1985, MNRAS 213, 889